Growth Modes

Today's solid state devices rely on the growth of sequences of many ultrathin epitaxial layers with atomically sharp interfaces and thickness control down to the monolayer (ML) level. A typical example is given by quantum well structures where alternating layers of wide bandgap and narrow bandgap semiconductors are grown to tailor the electronic properties by quantum confinement of charge carriers in the low bandgap regions. An example of equal practical interest is provided by stacking sequences of ferromagnetic layers separated by nonmagnetic spacer layers. By adjusting the spacer thickness, which must be below the spin coherence length (see *Giant Magnetoresistance*), the magnetic coupling between adjacent ferromagnetic layers can be controlled to be antiferromagnetic in the ground state, and ferromagnetic in the presence of an external field. Both states discern themselves by their strongly varying electrical conductivity perpendicular to the stacking sequence caused by scattering at the interfaces. This leads to a giant magnetoresistance effect which is used in magnetic hard disk read heads and sensors.

In both examples, and actually in most of the technologically relevant cases, the growth of perfectly flat, two-dimensional (2D) layers of materials A/B, and subsequently B/A, is a stringent requirement for functionality. The rare examples where a three-dimensional (3D) growth morphology is desired are semiconductor quantum dots, which may become relevant for optoelectronic devices or single electron transistors, or the surfaces used in heterogeneous surface chemical reactions, such as in catalysis or chemical sensors.

Epitaxial thin films and artificial multilayers are grown on solid single crystal surfaces with atomic monolayer thickness control either by chemical vapor deposition (CVD) (see *Chemical Vapor Deposition*) or by molecular beam epitaxy (MBE) (see *Molecular Beam Epitaxy*). In CVD, precursor molecules are thermally decomposed in a continuous flow oven in a background atmosphere of clean inert gas, whereas in MBE the surface is held in ultra high vacuum (UHV, typically at $p_{tot} \approx 1 \times 10^{-8}$ Pa) while being exposed to a vapor of molecules or atoms of the growing material. Controlling the growth morphology is a challenge in both fabrication techniques; it requires knowledge of both thermodynamics and of kinetics.

We will first discuss the classical thermodynamic approach to epitaxial thin film growth which led to the definition of the so-called growth modes. We then present the kinetic description of growth in which the film morphology is the result of the microscopic path taken by the system during growth. This path is determined by the hierarchy of rates of the single atom, cluster, or molecule displacements as compared to the deposition, desorption, and dissociation rates. We subsequently discuss growth manipulation by techniques mostly relying on kinetics that enable one to induce the often desired 2D growth. At the end there will be a brief discussion of the self-organized growth of equidistant semiconductor and metal nanostructures.

1. Thermodynamics—Growth Modes and Structural Mismatch

By the middle of the twentieth century the understanding of epitaxial growth was divided into three major schools of thought. Frank and van der Merwe used elasticity theory to derive the concept of a critical misfit below which monolayer-by-monolayer growth appears (Frank and van der Merwe 1949). Volmer and Weber, applying nucleation theory, assumed that crystalline films grew from 3D nuclei on the substrate and that their relative number and growth rate were determined by interfacial and surface free energies (Volmer and Weber 1926). The third model by Stranski and Krastanov was based on atomistic calculations and assumed that initially a few pseudomorphic 2D layers are formed, on top of which 3D crystals with their natural lattice constant will grow (Stranski and Krastanov 1938). Each of the three scenarios is observed, thus the three schools complement each other; they gave rise to the following labeling of the three growth modes of epitaxy:

(i) Frank–van der Merwe (FM) growth mode (2D morphology, layer-by-layer or step-flow growth)

(ii) Volmer–Weber (VW) growth mode (3D morphology, island growth)

(iii) Stranski–Kranstanov (SK) growth mode (initially 2D, after critical thickness, 3D morphology, layer-plus-island growth).

Unification of the three historical approaches to epitaxy, and prediction of the growth mode, were achieved by Bauer in considering the thermodynamic quantities involved in epitaxy, namely the three macroscopic surface tensions: γ_o, γ_i, and γ_s—the free energy per unit area at the overlayer–vacuum interface, the overlayer–substrate interface, and the substrate–vacuum interface, respectively (Bauer 1958). Bauer's concept evolves from comparing Figs. 1(a) and (b). If γ_o and γ_i are small compared to γ_s the system gains energy when totally covered by the overlayer, whereas, if not, it will only partly be covered (for a comprehensive review see Bauer 1984). For a film composed of n layers the criterion of case (i) (FM growth mode) is

$$\gamma_{o(n)} + \gamma_{i(n)} \leqslant \gamma_s \tag{1}$$

The n-dependence of γ_o reflects possible changes in lattice constant and/or structure at the overlayer surface. The thickness dependence of γ_i has its origins

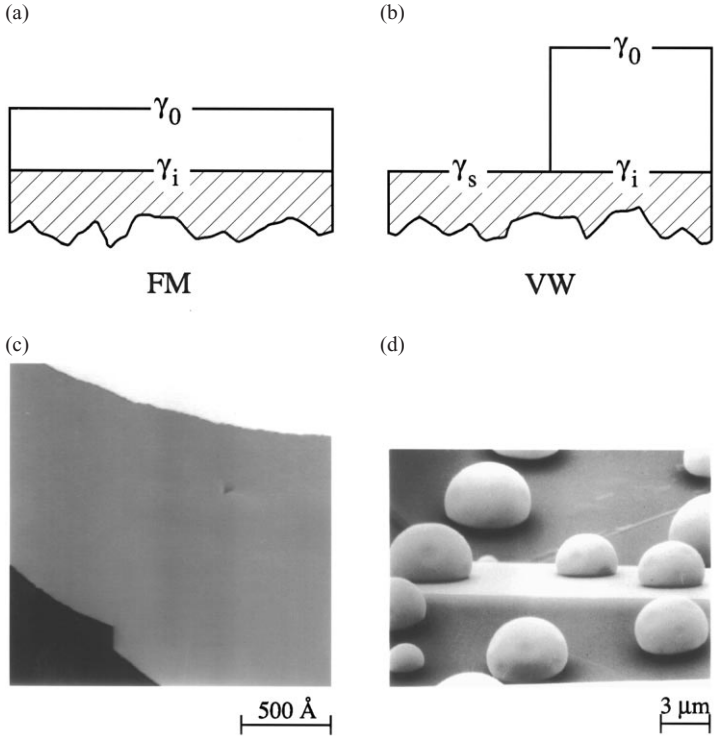

Figure 1
(a) Frank–van der Merwe (FM) growth compared with (b) Volmer–Weber (VW) growth (Zangwill 1988). (c) Perfectly 2D Ag film with Ag(111) lattice constant grown by depositing 25 ML Ag onto Pt(111) at 600 K and subsequent annealing to 800 K (Röder *et al.* 1997). (d) 3D Pb islands grown on highly oriented pyrolytic graphite (HOPG) imaged with an SEM (kindly provided by J. J. Métois).

in: (1) the true interface energy caused by the generally different crystallographic structure and/or lattice constant of overlayer and substrate, and (2) the volume strain accumulated in a pseudomorphic overlayer which is conveniently incorporated in $\gamma_{i(n)}$ (Bauer and van der Merwe 1986). The equality in Eqn. (1) holds for the trivial case of homoepitaxy which thus reveals the FM growth mode, if grown under conditions close to thermodynamic equilibrium. In the heteroepitaxial case the obvious condition for case (i) is that $\gamma_{o(n)} \ll \gamma_s$. The inequality in Eqn. (1) has to be large since in general $\gamma_{i(n)}$ is positive and non-negligible. The VW mode, case (ii), results if $\gamma_{o(n)} > \gamma_s$.

Examples of the cases (i) and (ii) are shown in Figs. 1(c) and (d). A 25 ML thick Ag film on Pt(111) grows perfectly flat, as evidenced by the scanning tunneling microscope (STM) image showing extended atomically flat terraces separated by monoatomic steps. The reason is that the surface free energy of Ag(111) ($\gamma_o = 1.17\,\mathrm{J\,m^{-2}}$) is sufficiently small compared to that of Pt(111) ($\gamma_s = 2.30\,\mathrm{J\,m^{-2}}$), and the strain containing interface energy of 25 ML is sufficiently small. The VW growth mode is realized for Pb ($\gamma_o = 0.60\,\mathrm{J\,m^{-2}}$; for a survey of metal surface free energies see Vitos *et al.* 1998) on graphite ($\gamma_s = 0.077\,\mathrm{J\,m^{-2}}$ at 1243 K (Abrahamson 1973)) as revealed by scanning electron microscopy (SEM). If one is close to thermodynamic equilibrium, such that the 3D island shape is comparable to that of liquid Pb droplets, the ratio of the surface free energies of Pb and HOPG is reflected in the contact angle θ formed by the Pb cluster surface and the substrate (Atkins 1990):

$$\cos\theta = \frac{\gamma_s - \gamma_i}{\gamma_o} \tag{2}$$

Structural mismatch of overlayer and substrate leads to a monotonic increase of volume strain energy in a 2D pseudomorphic layer with increasing film thickness n. Eqn. (1) implies that this leads to an unstable situation at a critical thickness n_c where $\gamma_{o(n)} + \gamma_{i(n)} > \gamma_s$ and the system switches from 2D to 3D growth morphology. This Stranski–Krastanov case (iii) presents a significant issue in the fabrication of coherently strained 2D device structures. On the other hand, the strain driven morphology transition is

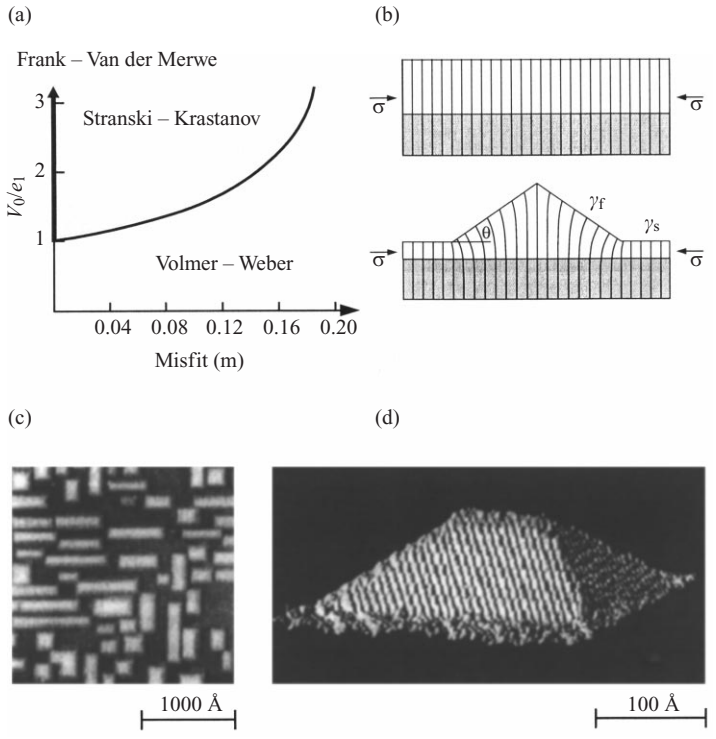

Figure 2
(a) Phase diagram of growth mode on an f.c.c. (100) surface in the substrate strength V_0/e_1 versus misfit m plane (Grabow and Gilmer 1988). (b) Coherently strained 2D film versus 3D pyramidal island situated on top of a planar wetting layer. The contact angle and surface energy of the inclined facet are θ and γ_f, respectively, while γ_s denotes the surface energy of the wetting layer. The compressive misfit stress is σ (Jesson *et al.* 1996). (c) and (d) STM images of "hut clusters" formed by Stranski–Krastanov growth of Ge on Si(100) (Mo *et al.* 1990).

beneficial for the self-assembly of quantum dots into arrays with sharp size and distance distributions (see Sect. 5).

The equilibrium configuration (structure and morphology) of a heteroepitaxial thin film is determined by the competition between the film–substrate interaction and the lateral adatom interaction in the film, describing the anisotropy of chemical bond strength parallel and perpendicular to the interface. Usual measures of these quantities are the isosteric heat of adsorption V_0 and the lateral adatom attraction e_1. The "phase diagram" derived from molecular dynamics simulations displayed in Fig. 2(a) reveals the expected growth modes in the V_0/e_1 versus misfit m plane.

The diagram shows that one can stabilize the FM growth mode only for so-called "strong" substrates, which impose their lattice constant onto the film atoms by a large corrugation of the interaction potential as compared to the stiffness of the lateral bonds of the adsorbate ($V_0/e_1 > 1$), and for small misfits. Films grow in VW mode down to very small misfits when lateral interactions dominate ($V_0/e_1 < 1$). If, for a given misfit, the influence of the substrate is increased on passes from VW to SK mode where a few 2D layers become thermodynamically stable.

There are two possible reasons for the transition from 2D to 3D morphology in the SK growth mode. The film material can grow in the first few monolayers in a crystallographic structure which differs appreciably from its own bulk (see for example f.c.c. Fe stabilized on Cu(100) (Straub *et al.* 1996)). In that case the SK mode will be accompanied by the crystallographic change to the bulk lattice structure of the film taking place at n_c. This induces an abrupt increase in free energy at the interface between the two crystal structures and changes the energy balance to favor 3D growth. The second possible reason is strain relief by the formation of "mounds." Figure 2(b) shows for the case of compressive strain, how mounds can adopt very efficiently their bulk lattice constant. When the strain energy is high the increase in surface area is more than counterbalanced. Figures 2(c) and (d) show atomic force microscopy (AFM) images of facetted pyramids forming in the Ge/Si(100) system which has 4.2% lattice misfit.

Compared to mounds, it is much harder to relieve strain in a perfectly 2D layer. In the best cases strained epitaxial layers exhibit a smooth transition in lattice constant from the substrate value over several weakly incommensurate phases (moiré structures or networks of partial surface dislocations) towards its bulk value (Brune and Kern 1997). Often, however, strain relief in a 2D layer implies the introduction of structural defects (LeGoues 1996) such as bulk dislocations which generally hamper functionality. Surface ripples (Cullis 1996) are an alternative way to relieve strain. With the increasing trend to use more highly strained material combinations, like InGaAs/GaAs and SiGe/Si, the suppression of the SK growth mode and the creation of defect-poor 2D layers in strained materials remains an important, largely unsolved issue.

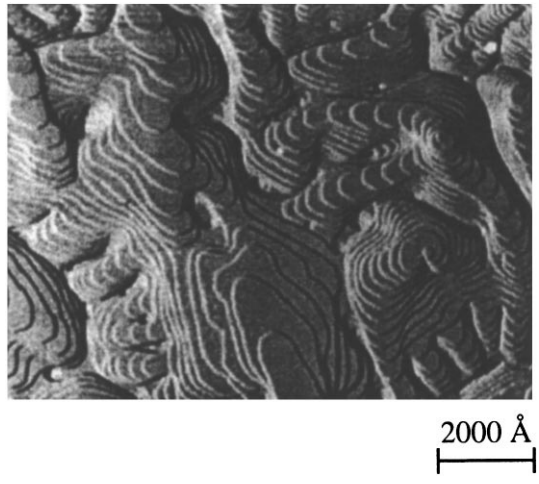

Figure 3
STM image showing the 3D growth morphology of 25 ML Ag grown on Ag(111) at 300 K (Vrijmoeth *et al.* 1994).

2. *Kinetics*

The classification into FM, VW, and SK growth modes, and the above considerations of strain relief, are only applicable for growth conditions close to thermodynamic equilibrium, i.e., at high substrate temperature and low deposition flux. However, detailed balance arguments imply that in equilibrium condensation and desorption, decay and binding of 2D clusters all have equal rates. Thus net growth requires being away from equilibrium. The degree to which one is away from equilibrium is determined by the supersaturation during growth. The term growth mode is justified at low supersaturation.

At high supersaturation the morphology is influenced by kinetics rather than by thermodynamics and the term growth mode should be replaced by growth morphologies which depend on the route taken by the system through the various reaction paths available during growth. An example of kinetically induced 3D morphology is observed in Fig. 3 displaying a system for which Eqn. (1) predicts the Frank–van der Merwe growth mode. Consequently, the surface shown in Fig. 3 becomes flat upon annealing to sufficiently high temperatures.

In many cases, however, the desired film morphology is metastable, motivating an interest in kinetics as the only means of controlling growth. Consider, for example, artificial multilayers. If material A perfectly wets material B, because $\gamma_A \ll \gamma_B$, then the text layer of material B will not be wetting the underlying A; it thus has to be stabilized in a 2D film by kinetics. Also, materials that are miscible will exhibit exchange, rendering the interface rough and ill defined. Exchange processes can be inhibited by growing at low temperature. We will discuss below how identification and experimental control of the important atomic processes during growth can be turned into recipes for growth manipulation.

The individual atomic processes involved in thin film MBE growth are shown in Fig. 4 (in the case of CVD growth there are in addition dissociation, diffusion, and desorption of the precursor molecules). Atoms are evaporated with flux F onto the substrate, where they are immediately thermalized. Their subsequent 2D diffusion rate D over the atomic terraces is given by Eqn. (3):

$$D = \frac{\langle r^2 \rangle}{4t} = \frac{d_{nn}^2 \nu_0}{4} e^{-E_m/kT} \tag{3}$$

where E_m is the activation energy for migration, i.e., the energy difference between the atom in the initial (often a hollow site) and in the transition state (often a bridge site). T is the substrate temperature and d_{nn} the surface nearest neighbor distance which equals the jump length.

The pre-exponential factor ν_0 is the vibrational frequency of the atom in the initial state; it is of the

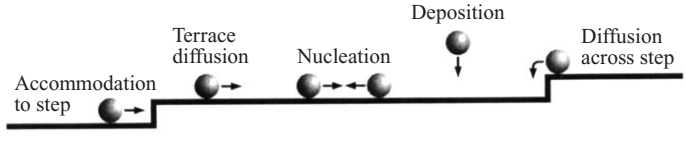

Figure 4
Elementary processes involved in island nucleation and thin film growth (simplified by one-dimensional projection).

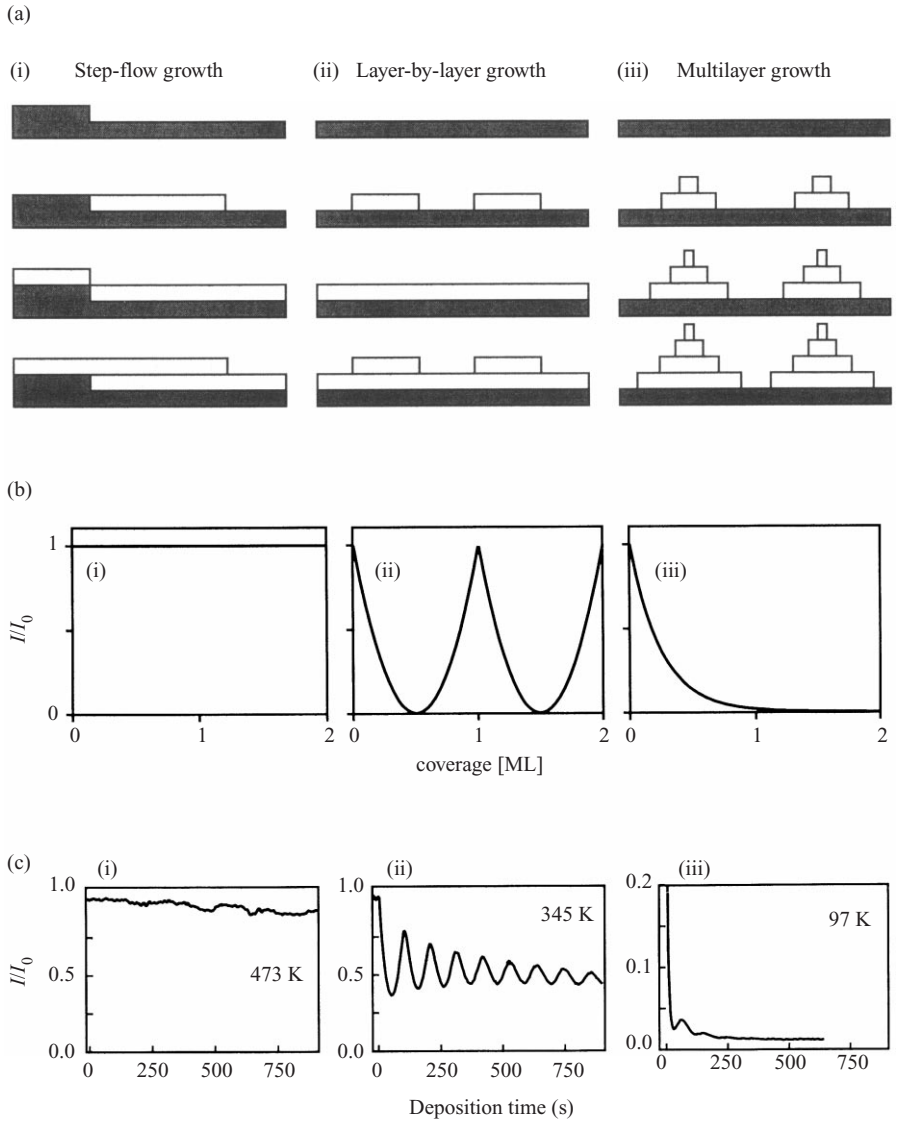

Figure 5
(a) Evolution of thin film growth morphology with coverage and (b) the corresponding normalized intensity of a diffraction signal under antiphase conditions for one atomic layer height difference. (c) Antiphase reflected intensity obtained from He atom scattering for Cu growth on a Cu(100) surface at various deposition temperatures (Jorritsma *et al.* 1997). Step-flow growth is observed at 473 K, layer-by-layer growth at 345 K, and kinetic roughening at 97 K.

order of $\nu_0 = 10^{13}$ Hz (for an account on surface diffusion see Tringides 1997). Similar relations to Eqn. (3) hold for all other thermally activated processes, like interlayer diffusion across monoatomic steps (Fig. 4). This process typically has a larger barrier than surface migration since it involves a lower coordinated transition state lying higher in energy.

The final film morphology in the kinetic growth regime is determined by the hierarchy of activation barriers which define the rates of atomic displacements, as compared to the deposition rate, which is the only parameter that introduces time. The detailed relationship between the macroscopic state of the system and all the microscopic processes is far from trivial. However, there are well-established general rules evolving from progress in the field, and for a few model systems the relationship between morphology and atomic diffusion rates can be unraveled (Brune

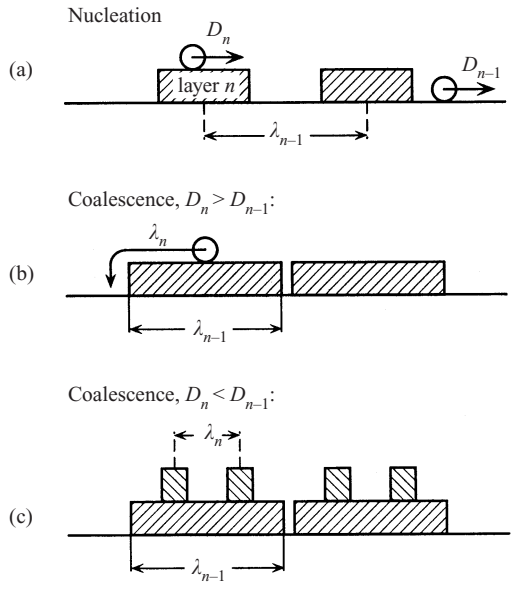

Figure 6
The concept of layer-dependent adatom mobilities introduced by Rosenfeld *et al*. (1998).

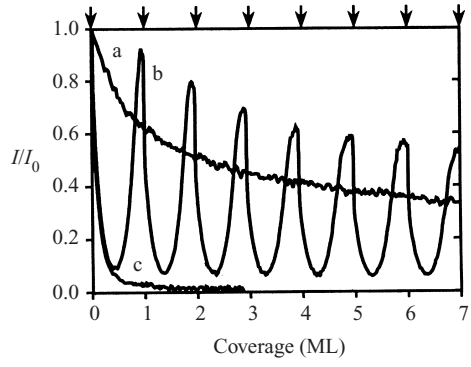

Figure 7
Growth manipulation to achieve layer-by-layer growth (Rosenfeld *et al*. 1998). Layer-by-layer oscillations (curve b) are observed in the antiphase He diffraction signal for Ag/Ag(111) at 300 K if the surface is subjected to a short sputter pulse each time a monolayer is completed (see arrows). Continuous sputtering while growing leads to 3D growth (curve c) as does continuous deposition (curve a).

1998). Here we discuss one simple case of the most relevant general rule relating the saturated density of nuclei n_x, from which the film grows, to the external parameters T and F (the suffix x refers to any nucleus size which is stable).

A direct relationship is established for the case where two monomers meet each other to form a stable and immobile nucleus (and for complete condensation into 2D islands); then mean-field nucleation theory (Venables 1973) and kinetic Monte–Carlo simulations (Bales and Chrzan 1994) consistently yield:

$$n_x = 0.25 \left(\frac{D}{F} \right)^{-1/3} \qquad (4)$$

Thus the mean distance a monomer travels before encountering one of its own or an existing nucleus is $\lambda \approx \sqrt{1/\pi n_x} \approx (D/F)^{1/6}$.

If λ is larger than the terrace width, no islands are formed since all atoms reach the ascending substrate steps to which they attach. This is the so-called step-flow growth at which the surface roughness remains constantly that of the substrate during growth. The surface roughness can be probed *in situ* by diffraction techniques using electrons, x rays, or a beam of helium atoms with thermal energy. In the last case a coherent He atom beam is adjusted with incident angle and wavelength such that the He atoms specularly reflected from a single monolayer of film atoms interfere out-of-phase with the He atoms reflected from the underlying layer. The reflected He intensity stays constant and high for step-flow growth (see Figs. 5(a)–(c)).

Periodic monolayer oscillations of the surface roughness appear when the film grows from nuclei which stay 2D during their growth until they coalesce (see Figs. 5(a)–(c) (ii)). This implies that all atoms deposited on top of the islands can descend. In this layer-by-layer growth the roughness has its maximum (and the reflected intensity its minimum) just before island coalescence and a minimum when an integer layer is completed. Growth oscillations are observed for our example of Cu(100) homoepitaxy when going to $T = 345$ K. Figures 5(a)–(c) (iii) show so-called kinetic roughening or multiplayer growth characterized by a monotonically increasing surface roughness. After the first layer nuclei have reached a certain size, atoms deposited on top can no longer descend quickly enough, leading to the critical monomer density on top of the island for second layer nucleation. (For dimers being stable nuclei it suffices to have two monomers that are present long enough on top of an island that they meet each other.) There are two possible reasons why atoms cannot descend sufficiently fast from the top of a 2D island. In the case of homoepitaxy the only reason for kinetic roughening is the extra barrier for edge descend, the so-called Ehrlich–Schwoebel barrier, E_s. This barrier is the reason why Ag grows three dimensionally at 300 K on Ag(111) (see Fig. 3, for Ag(111) $E_s = 220$ meV is substantial compared with $E_m = 100$ meV (Brune and Kern 1997)). The second reason brings us to the next section since it brings the possibility to manipulate growth.

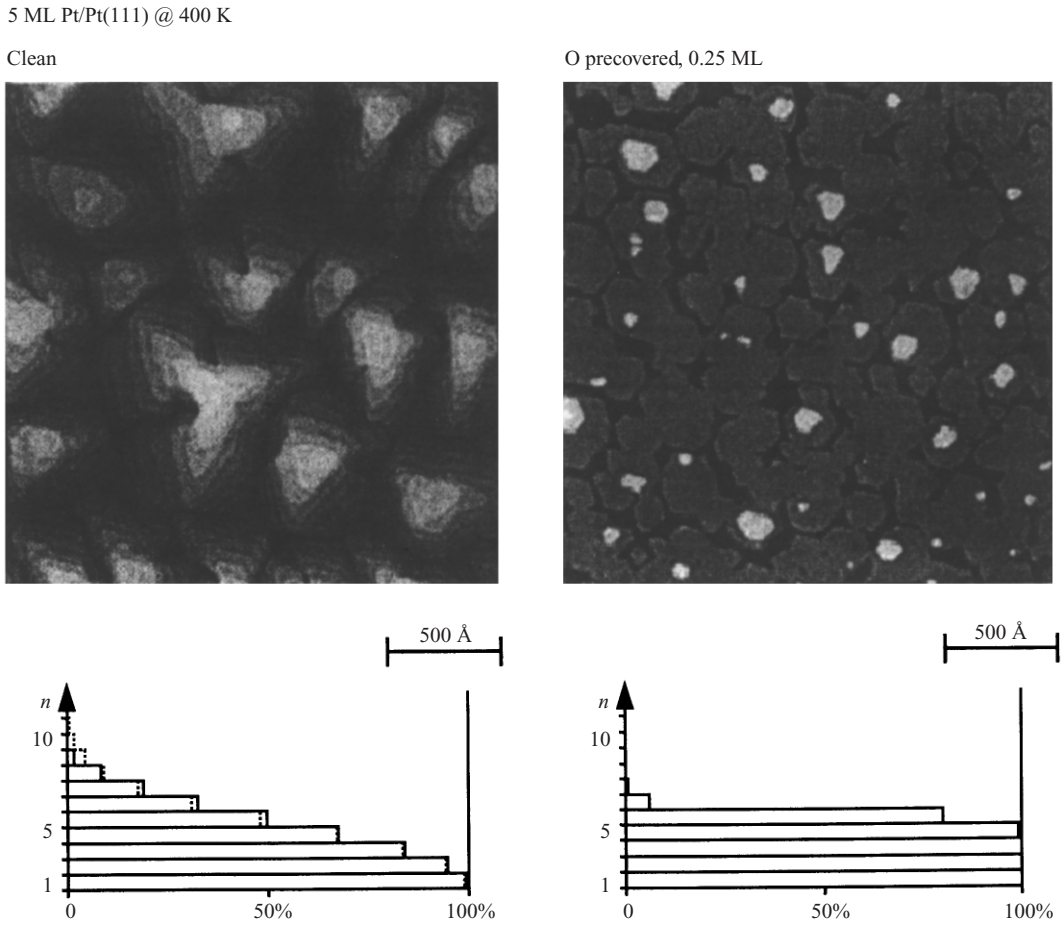

Figure 8
Surfactant effect of oxygen in Pt(111) homoepitaxy at 400 K growth temperature (Esch *et al*. 1994). The presence of chemisorbed oxygen leads to almost perfect layer-by-layer growth (right) whereas growth on the clean Pt surface is 3D with layer occupancies close to a Poisson distribution expected for inhibited interlayer mass transport.

3. Growth Manipulation

The necessary condition for layer-by-layer growth is that every atom deposited on top of an island can reach the descending step. The important condition is that it does descend before having the chance to create a stable cluster on top with one of its own. Both conditions have to be met at any stage of growth. The islands are largest just before coalescence. Assume we label the growing layer by n. The island diameter at coalescence equals the island separation and is λ_{n-1} which is given by Eqn. (4) through the mobility D_{n-1} of atoms of growing layer n on layer $n-1$ below (Fig. 6). If the mobility on top of layer n is larger or equal to that below, then $\lambda_n \geqslant \lambda_{n-1}$, and the atoms deposited on top reach the island edge at any stage of growth.

For homoepitaxy, D is layer independent and the atoms can reach the island edge, but only a limited number of times. If there is a small extra barrier for edge descend the system grows three-dimensionally. For heteroepitaxy, there are generally layer dependent mobilities resulting from layer-dependent surface structure and/or strain, which both have a strong effect on E_m and E_s. Strain can therefore promote layer-by-layer growth (Röder *et al*. 1997, Michely *et al*. 1996). The mobility on top of the growing layer can equally well be reduced by strain effects (the situation as depicted in Fig. 6(c)) which inhibits layer-by-layer growth, even in the absence of an extra barrier for interlayer mass transport.

The concept of layer-dependent mobilities described above opens up new ways of promoting layer-by-layer

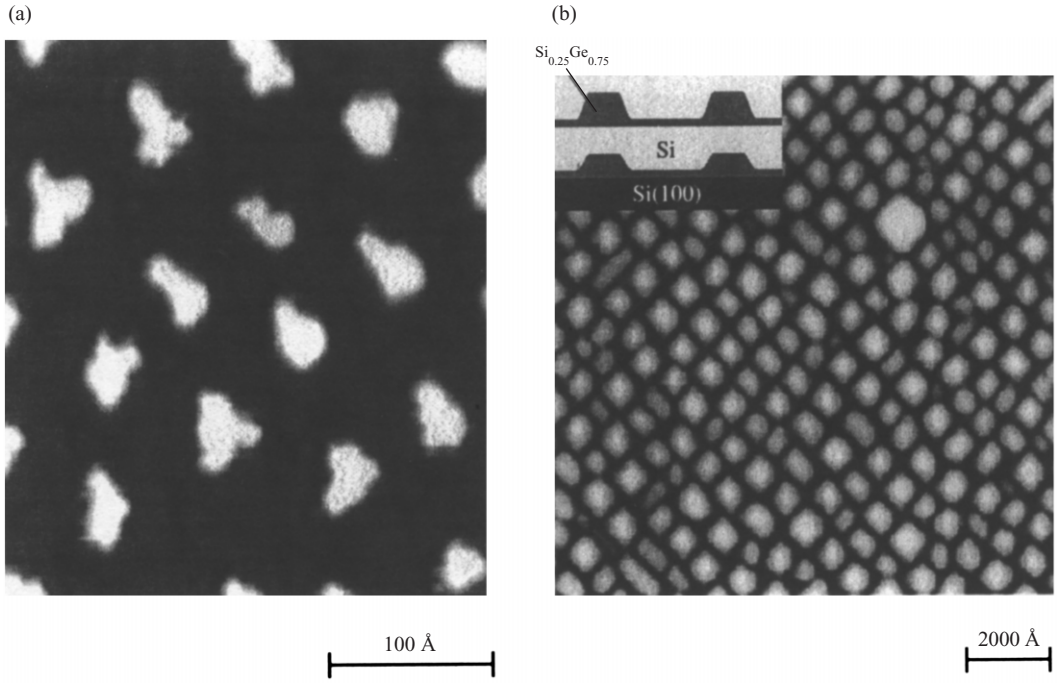

Figure 9
Self-organized growth of nanostructure arrays. (a) A hexagonal array of Ag islands (containing 62 ± 7 atoms each) created by kinetically controlled nucleation on the strain relief pattern (period 69 Å) of 2 ML Ag grown on Pt(111) (Brune *et al.* 1998). (b) $Si_{0.21}Ge_{0.75}$ quantum dots on Si(100) produced by periodic repetition of Stranski–Krastanov growth of dots as in Fig. 2 and subsequent capping with Si spacer layers. Elastic strain interactions through the spacer establish a correlation of nucleation sites between the buried dots and the ones grown on top. Repetition of the growth sequence (in the case of our figure 20 times) leads to highly ordered quantum dots arranged in a square array (Tersoff *et al.* 1996).

growth (Rosenfeld *et al.* 1998). The interlayer mass transport can be enhanced if the mobility on top of the growing layer is increased with respect to the one below. This increases the number of times an atom visits the descending step and thus its attempts to descend. In practice, variation of the mobilities on subsequent layers is achieved indirectly by variation of external parameters with monolayer period. The island density can, for example, be increased by brief ion bombardment during the initial nucleation phase ($\theta < 0.1$ ML) of each layer. After the sputter pulse, λ_{n-1} stays small since atoms travel only until they become captured by the existing nuclei.

The sputter pulse creates only very few defects on top of the nuclei, thus λ_n has its intrinsic high value giving rise to many attempts to descend. Figure 7 shows that this leads to pronounced layer-by-layer oscillations. The island density can similarly be decreased by lowering T, or increasing F during the initial nucleation phase (note that T has an exponential effect, whereas F enters linearly in Eqn. (4)). All three methods were shown to promote layer-by-layer growth (Rosenfeld *et al.* 1998).

The above method of kinetic growth improvement is indirect as it does not alter the step-edge barrier itself. One can directly reduce the effective E_s value by suitable additives, or by changes in the structure of island edges enhancing the fraction of step sites (kinks), where E_s is small. An example of the first case is shown in Fig. 8, here oxygen was chemisorbed as a surfactant to promote layer-by-layer growth in Pt(111) homoepitaxy. The clean Pt(111) system shows kinetic roughening with 3D islands and layer occupancies reminiscent of very little interlayer mass transport. The $p(2 \times 2)$ oxygen precovered substrate shows perfect layer-by-layer growth with only three open layers.

A requirement of a surfactant is that it floats up onto the surface of the growing layer. Although surfactant-promoted growth has been the subject of intense research, the exact way that surfactants work is still a matter of debate, and is certainly also system specific. In our example the surfactant only reduces E_s (Esch *et al.* 1994). It is likely, however, that the moment when the surfactant floats up is abrupt and may well coincide with coalescence. In that case a surfactant would also induce layer-dependent mobilities.

So far, the technological application of surfactant-promoted growth is limited by the difficulty of removing the floating adsorbed overlayer from the deposited film after growth is completed. This favors the use of simple adsorbed gases (like O_2 in Fig. 8) which often can more easily be removed than the classical surfactants As, Sb, or Pb.

4. Self-organized Growth

For applications in heterogeneous catalysis, sensors, electronic devices, or for fundamental studies, large number densities of equally sized and equally spaced metallic or semiconductor nanostructures are anticipated most. Fabrication by lithographic techniques pushes e-beam patterning to its limits and is often not possible because of the materials that need to be studied, because of resolution limits, or because of the requirements of material purity. Local probe assisted fabrication has created fascinating structures ideally suited to test our ideas, for example, about quantum mechanics, on an object of our choice, but it has the disadvantage of being sequential. Therefore attempts were made to use the self-organized growth of nanostructure arrays (see *Semiconductor Nanostructures, Self-organization of*).

Figure 9 shows two successful ways of generating equally spaced nanostructures with very narrow size distributions. In the metal case a strain relief pattern was generated by growing a thin mismatched film on an f.c.c.(111) surface. In many cases strain relief on this surface orientation leads to well-ordered superstructures with a lattice constant $1/m$ (Brune *et al.* 1998). The superstructure was used as a template surface to grow equally spaced islands through kinetically controlled growth. The adatom density and thus the nucleation probability is highest at the locations in the superstructure unit cell where atoms are most strongly bound. By choosing the temperature such that λ is sufficient to reach these locations, but intercell diffusion is suppressed, exactly one island per unit cell can be nucleated. In this approach the island size is controlled by the coverage and the distance by the misfit of the two materials used to create the template (Brune *et al.* 1998).

The second approach uses strain mediated nucleation on top of buried islands through a spacer layer. $Si_x\,Ge_{1-x}$ quantum dots are grown by the SK mode on Si(100), as the pure Ge "mounds" in Figs. 1(c) and (d). Subsequently, these "hut" clusters are capped by Si. The Si layer is compressively strained on top of a buried quantum dot inducing a high probability for nucleation of a new quantum dot. If, by statistical fluctuations, two buried dots are too far apart there will be a high probability of nucleating one in between them. If two buried dots are too close, the strain fields in the Si spacer overlap and only one nucleates on top. Repetition of the growth sequence, quantum dots–spacer layer, yields to increased order as evidenced by Fig. 9(b). The best size distributions currently achieved using both techniques are characterized by $\sigma = 12\%$ standard deviation in the island area.

5. Summary

Thermodynamic arguments have led to a definition of three epitaxial growth modes. The desired thin film morphology and that of artificial multilayers are quite often not realized by growing close to thermodynamic equilibrium. The kinetics of epitaxy offers many ways of creating the desired film morphology in a metastable state, be it 2D layers by kinetically promoted layer-by-layer growth or nanostructure arrays by kinetically controlled nucleation.

See also: Surfaces: Reconstruction; Thin-film Growth: Phase Transition

Bibliography

Abrahamson J 1973 The surface energies of graphite. *Carbon* **11**, 337–62

Atkins P W 1990 *Physical Chemistry*, 4th edn. Oxford University Press, Oxford

Bales G S, Chrzan D C 1994 Dynamics of irreversible island growth during submonolayer epitaxy. *Phys. Rev. B* **50**, 6057–67

Bauer E 1958 Phänomenologische Theorie der Kristallabscheidung an Oberflächen I. *Z. Kristallogr.* **110**, 372–94

Bauer E 1984 Metals on metals. In: King D A, Woodruff D P (eds.) *The Chemical Physics of Solid Surfaces and Heterogeneous Catalysis*, Vol. 3B, *Chemisorption Systems*, *Part B*. Elsevier Science, Amsterdam, pp. 1–57

Bauer E, Van der Merwe J H 1986 Structure and growth of crystalline superlattices: From monolayer to superlattice. *Phys. Rev. B* **33**, 3657–71

Brune H 1998 Kinetics of nucleation and aggregation in metal epitaxy. *Surf. Sci. Rep.* **31**, 121–230

Brune H, Giovannini M, Bromann K, Kern K 1998 Self-organized growth of nanostructure arrays. *Nature* **394**, 451–3

Brune H, Kern K 1997 Heteroepitaxial metal growth: the effects of strain. In: King D A, Woodruff D P (eds.) *The Chemical Physics of Solid Surfaces and Heterogeneous Catalysis*, Vol. 8 *Growth and Properties of Ultrathin Epitaxial Layers*. Elsevier Science, Amsterdam, pp. 149–206

Cullis A G 1996 Strain-induced modulations in the surface morphology of heteoepitaxial layers. *Mater. Res. Soc. Bull.* **21**, 21–6

Esch S, Hohage M, Michely T, Comsa G 1994 Origin of oxygen induced layer-by-layer growth in homoepitaxy on Pt(111). *Phys. Rev. Lett.* **72**, 518–21

Frank F C, van der Merwe J H 1949 One-dimensional dislocations. II. Misfitting monolayers and oriented overgrowth. *Proc. R. Soc. London A* **198**, 216–25

Grabow M H, Gilmer G H 1988 Thin film growth modes, wetting and cluster nucleation. *Surf. Sci.* **194**, 333–46

Jesson D E, Chen K M, Pennycook S J 1996 Kinetic pathways to strain relaxation in the Si–Ge system. *Mater. Res. Soc. Bull.* **21**, 31–7

Jorritsma L C, Bijnagte M, Rosenfeld G, Poelsema B 1997 Growth anisotropy and pattern formation in metal epitaxy. *Phys. Rev. Lett.* **78**, 911–4

LeGoues F K 1996 The effect of strain on the formation of dislocations at the SiGe/Si interface. *Mater. Res. Soc. Bull.* **21**, 21–6

Michely T, Hohage M, Esch S, Comsa G 1996 The effect of surface reconstruction on the growth mode in homoepitaxy. *Surf. Sci.* **349**, L89–94

Mo Y W, Savage D E, Swartzentruber B S, Lagally M G 1990 Kinetic pathway in Stranski–Krastanov growth of Ge on Si(001). *Phys. Rev. Lett.* **65**, 1020–3

Röder H, Bromann K, Brune H, Kern K 1997 Strain mediated two-dimensional growth kinetics in metal heteroepitaxy: Ag/Pt(111). *Surf. Sci.* **376**, 13–31

Rosenfeld G, Comsa C, Poelsema B 1998 The concept of two mobilities for growth manipulation. In: Zhang Z, Lagally M G (eds.) *Morphological Organization in Epitaxial Growth and Removal*, Vol. 14 *Series in Direction in Condensed Matter Physics*. World Scientific, Singapore, pp. 349–66

Stranski I N, Krastanov L 1938 Zur Theorie der orientierten Ausscheidung von Ionenkristallen aufeinander. *Sitzungsbericht Akademie der Wissenschaften Wien, Math.-naturwiss. Kl. IIb* **146**, 797–810

Straub M, Vollmer B, Kirschner J 1996 Surface magnetism of ultrathin γ-Fe films investigated by nonlinear magneto-optical Kerr effect. *Phys. Rev. Lett.* **77**, 743–6

Tersoff J, Teichert C, Lagally M G 1996 Self-organization in growth of quantum dot superlattices. *Phys. Rev. Lett.* **76**, 1675–8

Tringides M C 1997 *Surface Diffusion–Atomistic and Collective Processes*, in NATO Advanced Science Institute, Series B: Physics, Vol 360, Plenum Press, New York

Venables J A 1973 Rate equation approaches to thin film nucleation Kinetics. *Philos. Mag.* **17**, 697–738

Vitos L, Ruban A V, Skriver H L, Kollár J 1998 The surface energy of metals. *Surf. Sci.* **411**, 186–202

Volmer M, Weber A 1926 Keimbildung in übersättigten Gebilden. *Z. physik. Chem.* **119**, 277–301

Vrijmoeth J, van der Vegt H A, Meyer J A, Vlieg E, Behm R J 1994 Surfactant-induced layer-by-layer growth of Ag on Ag(111): origins and side effects. *Phys. Rev. Lett.* **72**, 3843–6

Zangwill A 1988 *Physics at Surfaces*. Cambridge University Press, New York

H. Brune

Encyclopedia of Materials: Science and Technology
ISBN: 0-08-0431526
pp. 3683–3693